

A novel multiple-stage antimalarial agent that inhibits protein synthesis

Beatriz Baragaña¹, Irene Hallyburton¹, Marcus C. S. Lee^{2†}, Neil R. Norcross¹, Raffaella Grimaldi¹, Thomas D. Otto³, William R. Proto³, Andrew M. Blagborough⁴, Stephan Meister⁵, Grennady Wirjanata⁶, Andrea Ruecker⁴, Leanna M. Upton⁴, Tara S. Abraham², Mariana J. Almeida², Anupam Pradhan⁷, Achim Porzelle¹, María Santos Martínez⁸, Judith M. Bolscher⁹, Andrew Woodland¹, Suzanne Norval¹, Fabio Zuccotto¹, John Thomas¹, Frederick Simeons¹, Laste Stojanovski¹, Maria Osuna-Cabello¹, Paddy M. Brock⁴, Tom S. Churcher⁴, Katarzyna A. Sala⁴, Sara E. Zakutansky⁴, Maria Belén Jiménez-Díaz⁸, Laura Maria Sanz⁸, Jennifer Riley¹, Rajshekhar Basak², Michael Campbell¹⁰, Vicky M. Avery¹¹, Robert W. Sauerwein⁹, Koen J. Dechering⁹, Rintis Noviyanti¹², Brice Campo¹³, Julie A. Frearson¹, Iñigo Angulo-Barturen⁸, Santiago Ferrer-Bazaga⁸, Francisco Javier Gamó⁸, Paul G. Wyatt¹, Didier Leroy¹³, Peter Siegl¹³, Michael J. Delves⁴, Dennis E. Kyle⁷, Sergio Wittlin¹⁴, Jutta Marfurt⁶, Ric N. Price^{6,15}, Robert E. Sinden⁴, Elizabeth A. Winzeler⁵, Susan A. Charman¹⁰, Lidiya Bebrevska¹³, David W. Gray¹, Simon Campbell¹³, Alan H. Fairlamb¹, Paul A. Willis¹³, Julian C. Rayner³, David A. Fidock^{2,16}, Kevin D. Read¹ & Ian H. Gilbert¹

There is an urgent need for new drugs to treat malaria, with broad therapeutic potential and novel modes of action, to widen the scope of treatment and to overcome emerging drug resistance. Here we describe the discovery of DDD107498, a compound with a potent and novel spectrum of antimalarial activity against multiple life-cycle stages of the *Plasmodium* parasite, with good pharmacokinetic properties and an acceptable safety profile. DDD107498 demonstrates potential to address a variety of clinical needs, including single-dose treatment, transmission blocking and chemoprotection. DDD107498 was developed from a screening programme against blood-stage malaria parasites; its molecular target has been identified as translation elongation factor 2 (eEF2), which is responsible for the GTP-dependent translocation of the ribosome along messenger RNA, and is essential for protein synthesis. This discovery of eEF2 as a viable antimalarial drug target opens up new possibilities for drug discovery.

The World Health Organization estimates that there were approximately 200 million clinical cases and 584,000 deaths from malaria in 2013, predominantly among children and pregnant women in sub-Saharan Africa¹. The malaria parasite has developed resistance to many of the current drugs, including emerging resistance to the core artemisinin component of artemisinin-based combination therapies that constitute current first-line therapies². To support the current treatment and eradication agenda³, there are several requirements for new antimalarials: novel modes of action with no cross-resistance to current drugs; single-dose cures; activity against both the asexual blood stages that cause disease and the gametocytes responsible for transmission; compounds that prevent infection (chemoprotective agents); and compounds that clear *Plasmodium vivax* hypnozoites from the liver (anti-relapse agents)⁴.

Discovery of a novel antimalarial

A phenotypic screen of the Dundee protein kinase scaffold library⁵ (then 4,731 compounds) was performed against the blood stage of the multi-drug-sensitive *Plasmodium falciparum* 3D7 strain. A compound series from this screen, based on a 2,6-disubstituted quinoline-4-carboxamide scaffold, had sub-micromolar potency against

the parasites, but suffered from poor physicochemical properties. Chemical optimization (Fig. 1 and Extended Data Fig. 1) led to DDD107498 with improved physicochemical properties (Tables 1 and 2 in Supplementary Methods) and a 100-fold increase in potency. The key stages involved were replacing the bromine with a fluorine atom to reduce molecular mass and lipophilicity; replacing the 3-pyridyl substituent with an ethyl-pyrrolidine group; and addition of a morpholine group via a methylene spacer. Initial cost-of-goods estimates and likely human dose projections suggest a low cost (approximately US\$1 per treatment), which is important, given that most of the patient population is living in poverty.

Blood-stage activity and developability

DDD107498 showed excellent activity against 3D7 parasites: 50% effective inhibitory concentration (EC₅₀) = 1.0 nM (95% confidence interval (CI) 0.8–1.2 nM); EC₉₀ = 2.4 nM (95% CI 2.0–2.9 nM); EC₉₉ = 5.9 nM (95% CI 4.5–7.6 nM), (*n* = 39). It was also almost equally active against several drug-resistant strains (Extended Data Fig. 2a)⁶. Furthermore, DDD107498 was more potent than artesunate in *ex vivo* assays against a range of clinical isolates of both *P. falciparum* (median EC₅₀ = 0.81 nM (range 0.29–3.29 nM), *n* = 44) and

¹Drug Discovery Unit, Division of Biological Chemistry and Drug Discovery, College of Life Sciences, University of Dundee, Dundee DD1 5EH, UK. ²Department of Microbiology and Immunology, Columbia University College of Physicians and Surgeons, New York, New York 10032, USA. ³Malaria Programme, Wellcome Trust Sanger Institute, Wellcome Trust Genome Campus, Cambridge CB10 1SA, UK.

⁴Department of Life Sciences, Imperial College, London SW7 2AZ, UK. ⁵University of California, San Diego, School of Medicine, 9500 Gilman Drive 0760, La Jolla, California 92093, USA. ⁶Global Health and Tropical Medicine Division, Menzies School of Health Research, Charles Darwin University, PO Box 41096, Casuarina, Darwin, Northern Territory 0811, Australia. ⁷Department of Global Health, College of Public Health University of South Florida, 3720 Spectrum Boulevard, Suite 304, Tampa, Florida 33612, USA. ⁸GlaxoSmithKline, Tres Cantos Medicines Development Campus-Diseases of the Developing World, Severo Ochoa 2, Tres Cantos 28760, Madrid, Spain. ⁹TropiQ Health Sciences, Geert Groteplein 28, Huispost 268, 6525 GA Nijmegen, The Netherlands. ¹⁰Centre for Drug Candidate Optimisation, Monash University, 381 Royal Parade, Parkville, Victoria 3052, Australia. ¹¹Eskitis Institute, Brisbane Innovation Park, Nathan Campus, Griffith University, Queensland 4111, Australia.

¹²Malaria Pathogenesis Laboratory, Eijkman Institute for Molecular Biology, Jalan Diponegoro 69, 10430 Jakarta, Indonesia. ¹³Medicines for Malaria Venture, PO Box 1826, 20 route de Pre-Bois, 1215 Geneva 15, Switzerland. ¹⁴Swiss Tropical and Public Health Institute, Socinstrasse 57, 4051 Basel, Switzerland. ¹⁵Centre for Tropical Medicine and Global Health, Nuffield Department of Medicine, University of Oxford, Oxford OX3 7LJ, UK. ¹⁶Division of Infectious Diseases, Department of Medicine, Columbia University College of Physicians and Surgeons, New York, New York 10032, USA.

†Present address: Wellcome Trust Sanger Institute, Wellcome Trust Genome Campus, Hinxton, Cambridge CB10 1SA, UK.

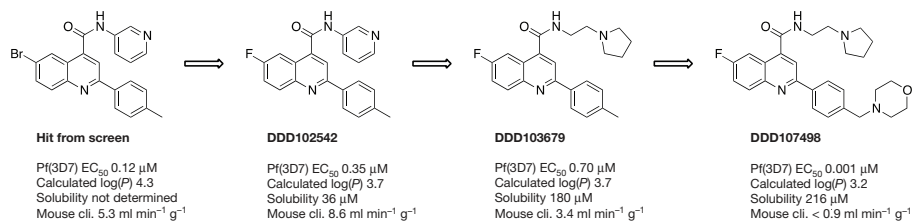


Figure 1 | Chemical evolution of DDD107498 from the phenotypic hit. Calculated log(P), calculated log(partition coefficient); Solubility, solubility in water; Mouse cli., intrinsic clearance in mouse liver microsomes.

P. vivax (median EC₅₀ = 0.51 nM (range 0.25–1.39 nM), *n* = 28) collected from patients with malaria from southern Papua, Indonesia, a region where high-grade multidrug-resistant malaria is endemic for both species (Extended Data Fig. 2b)^{7,8}. In contrast, the compound was not toxic to human cells (MRC5 and Hep-G2 cells) at much higher concentrations (>20,000-fold selectivity; Extended Data Fig. 2c).

DDD107498 showed good drug-like properties: metabolic stability when incubated with hepatic microsomes or hepatocytes from several species; good solubility in a range of different media; and low protein binding (Tables 1 and 2 in Supplementary Methods). DDD107498 displayed excellent pharmacokinetic properties in preclinical species, including good oral bioavailability (an important prerequisite for use in resource-poor settings) and long plasma half-life (important for single-dose treatment and chemoprotection) (Extended Data Table 1a).

DDD107498 was very active in several mouse models of malaria, with comparable or greater efficacy than current antimalarials (Extended Data Table 1b). DDD107498 had a 90% reduction in parasitaemia (ED₉₀) of 0.57 mg per kg (body weight) after a single oral dose in mice infected with the rodent parasite *Plasmodium berghei*. Efficacy was also tested in NOD-*scid* IL-2R_{null} mice engrafted with human erythrocytes and infected with *P. falciparum* strain 3D7^{0087/N9} (Fig. 2a)⁹. When orally dosed daily for 4 days, the ED₉₀ on day 7 after infection was 0.95 mg per kg per day. Blood sampling from the infected SCID (severe combined immunodeficiency) mice suggested a minimum parasiticidal concentration for DDD107498 of 10–13 ng ml⁻¹ for asexual blood-stage infections.

The effects of DDD107498 on circulating parasites in the SCID mouse model could be observed in one replication cycle (48 h) and led to trophozoites with condensed cytoplasm (Extended Data Fig. 3). Stage specificity studies using synchronized cultures showed that, at a concentration of 4 nM for 24 h, DDD107498 led to (1) from the ring stage, formation of abnormal trophozoites; (2) from the trophozoite stage, prevention of schizont formation with a 50% reduction in parasites, indicative of cidal activity; and (3) from the schizont stage, prevention of ring formation with a 98% reduction in parasites, indicative of cidal activity (Extended Data Fig. 3b, c).

DDD107498 showed a similar parasite killing profile both *in vitro* (Fig. 2b, c) and *in vivo* (Fig. 2a), which is supportive of a common mode of action in cellular and animal models of disease. Using a parasite reduction rate assay¹⁰ there was a lag of about 24–48 h, during which time the effects of the compounds were reversible following wash-out. Rapid killing occurred after parasites had been exposed to DDD107498 for more than 48 h (Fig. 2b, c).

All these experiments suggest for the blood-stage form that treatment with DDD107498 prevented development of trophozoites and schizonts and, at least in the case of schizonts, caused rapid killing. Any ring-stage parasites only developed as far as abnormal trophozoites, which appeared to survive for about 48 h under drug pressure, but were then killed.

In safety studies, DDD107498 showed no clinically relevant inhibition of any of the major human cytochrome P450 (CYP) isoforms and

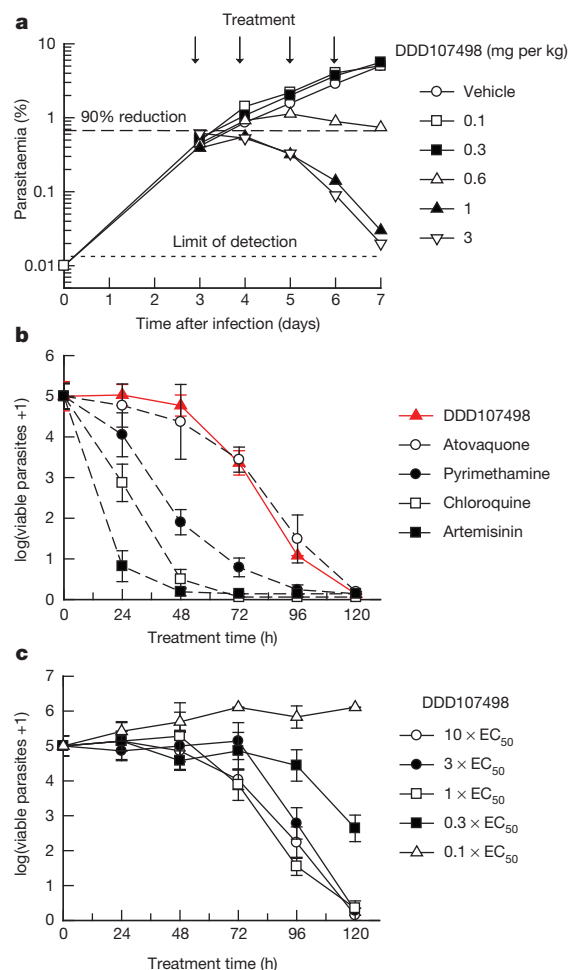


Figure 2 | Efficacy studies and parasite killing rate. **a**, *In vivo* activity against *P. falciparum* in NOD-*scid* IL-2R_{null} mice. Six mice were used, each serially sampled. The variability of cytometry for repeated acquisitions of a sample is less than 2–3%. The percentage of parasitaemia was calculated by acquiring a minimum number of 500 parasitized erythrocytes. An independent experiment with three further mice was performed to confirm the ED₉₀. **b**, Determination of the *in vitro* killing rate of DDD107498. The *in vitro* parasite reduction rate assay was used to determine onset of action and rate of killing as previously described¹⁰. *P. falciparum* was exposed to DDD107498 at a concentration corresponding to 10 × EC₅₀. The number of viable parasites at each time point was determined as described¹⁰. Four independent serial dilutions were done with each sample to correct for experimental variation; error bars, s.d. Previous results reported on standard antimalarials tested at 10 × EC₅₀ using the same conditions are shown for comparison¹⁰. **c**, The *in vitro* parasite reduction rate assay was used to determine the minimal concentration of compound needed for achieving maximal killing effects. Parasites were exposed to DDD107498 at concentrations of 0.1, 0.3, 1, 3 and 10 × EC₅₀ using conditions described above. Error bars, s.d. Concentrations of DDD107498 of 1 × EC₅₀ are sufficient to produce maximal killing effects on treated parasites.

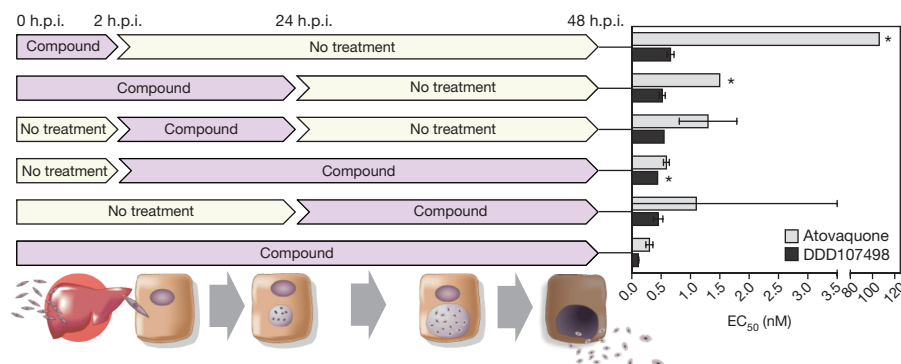


Figure 3 | *In vitro* activity of DDD107498 against *P. berghei* liver stages. Each experiment was the average of four technical replicates; h.p.i., hours post-infection. Bars, 95% CI. *More than one curve fitting possible.

CYP450 induction risk was low (Table 3 in Supplementary Methods), indicating a low risk of clinical drug–drug interactions. DDD107498 is non-mutagenic and has very weak inhibitory potencies on I_{Kr} (hERG) and other ion channels, indicating a very low risk for adverse cardiovascular activity. Given its potency, long half-life observed in preclinical species, and safety margins from a rat 7-day toxicology study, DDD107498 has potential both for single-dose treatment and for once-weekly chemoprotection¹¹.

Activity against other life-cycle stages

Intra-hepatocytic parasites (liver schizont stages) are the first stage of human infection after injection of sporozoites by anopheline mosquitoes. Compounds active against this stage have potential for use in chemoprotection. DDD107498 showed an $EC_{50} \approx 1$ nM against the liver schizont forms of *P. berghei* and *Plasmodium yoelii*¹². DDD107498 was active when dosed for only 2 h during the initial infection (hepatocyte invasion) of the liver cells (Fig. 3). In contrast, atovaquone (clinically used for chemoprotection in combination with proguanil) had a much reduced activity during this period ($EC_{50} \approx 106$ nM versus 0.3 nM for continuous treatment). Further, DDD107498 showed equivalent potency against the *P. berghei* liver stage when added after initial infection had been established (Fig. 3). This suggests that intermittent treatment may be sufficient for chemoprotection. To assess chemoprotective potential *in vivo*, mice were treated with DDD107498 2 h before being infected with luciferase-expressing *P. berghei* sporozoites (Extended Data Fig. 4). At a dose of 3 mg per kg, DDD107498 was fully curative with no sign of parasitaemia after 30 days. Thus, DDD107498 demonstrates potent chemoprotection using *in vitro* and *in vivo* models, where blood sampling from the mice during the experiment suggests a minimum parasitocidal concentration of 15–20 ng ml⁻¹.

The parasite erythrocytic form differentiates into the asymptomatic male and female gametocytes (stages I–V) within the human host. Mature stage V gametocytes are infective to mosquitoes, but are not eliminated by the majority of current antimalarial agents, and remain circulating in the human bloodstream for up to 3 weeks, long after the disappearance of clinical symptoms of malaria^{13,14}. After ingestion by the mosquito, gametocytes differentiate into gametes. DDD107498 potently inhibited both male and female gamete formation from the gametocyte stage at similar concentrations (1.8 nM (95% CI 1.6–2.1 nM) and 1.2 nM (95% CI 0.8–1.6 nM) respectively; Extended Data Fig. 5), indicating that it is an extremely potent inhibitor of the functional viability of both male and female mature gametocytes¹⁵. In line with this, DDD107498 blocked transmission, as determined by the standard membrane feeding assay. In this assay, parasite cultures containing *P. falciparum* stage V gametocytes were exposed to compound for 24 h before mosquito feeding. DDD107498 blocked subsequent oocyst development in the mosquito (measured

after 7 days) with an EC_{50} of 1.8 nM. At a baseline oocyst intensity of 27 oocysts per mosquito in the DMSO controls, prevalence of infection was inhibited, with an EC_{50} of 3.7 nM, as measured by the number of infected mosquitoes. Repeating the standard membrane feeding assay in which DDD107498 was added at the moment of mosquito feeding gave an EC_{50} of 10 nM, indicating potent activity against the parasite sexual stages that develop in the mosquito midgut (Extended Data Fig. 5)¹⁶.

A *P. berghei* mouse-to-mouse^{17,18} model was additionally used to examine transmission blockade. Mice were infected with *P. berghei* (PbGFPCON507)¹⁹, and then treated orally with compound 24 h before mosquitoes took a direct blood meal¹⁷. After a 3 mg per kg dose of DDD107498, a 90.7% reduction in infected mosquitoes and a 98.8% reduction in oocysts per midgut was observed at day 10 compared with mosquitoes fed on untreated mice (Extended Data Fig. 6). A corresponding reduction in sporozoite intensity and prevalence was observed (93.8% and 88.6% respectively). Mosquitoes previously fed on infected, drug-treated mice were allowed to feed on uninfected mice¹⁷. Testing a range of mosquito biting rates, we observed a mean reduction of 89.5% (95% CI 71.4–100) in the number of mice that developed blood-stage infection compared with mice bitten by mosquitoes that had fed on non-drug-treated infected mice. The overall effectiveness of an intervention over a round of transmission (from mouse to mosquito to mouse) can be quantified by estimating its ability to reduce the basic reproductive number (R_0). This has been termed the ‘effect size’ of an intervention. By fitting data from the mouse-to-mouse assay to a chain binomial model we can estimate the effect size of the intervention¹⁷, assessing the ability of DDD107498 usage to reduce the basic reproductive number R_0 (assuming 100% coverage). Our results estimate an effect size of 90.5% (95% CI 78.3–94.2), suggesting that DDD107498 is capable of acting as a potent transmission-blocking drug over multiple transmission settings within a field context¹⁸. The combination of these key *in vitro* and *in vivo* assays demonstrates the very strong potential of DDD107498 for blocking transmission; importantly, the required doses are likely to be similar to those required for treatment of blood-stage malaria.

DDD107498 targets PfeEF2

To determine the molecular target for DDD107498, asexual blood-stage *P. falciparum* were cultured in the presence of DDD107498 at $5 \times EC_{50}$, until parasites became resistant (Extended Data Table 2)²⁰. Resistance was obtained in the 3D7 (drug-sensitive) and 7G8 and Dd2 (multi-drug-resistant) strains, with minimum inocula of 10^7 , 10^7 and 10^6 parasites respectively. Genomic DNA was extracted from resistant lines and whole-genome sequencing of ten drug-resistant lines identified shared mutations in one gene, which were not present in the parental lines: Pf3D7_1451100 (Supplementary Data 1). This gene

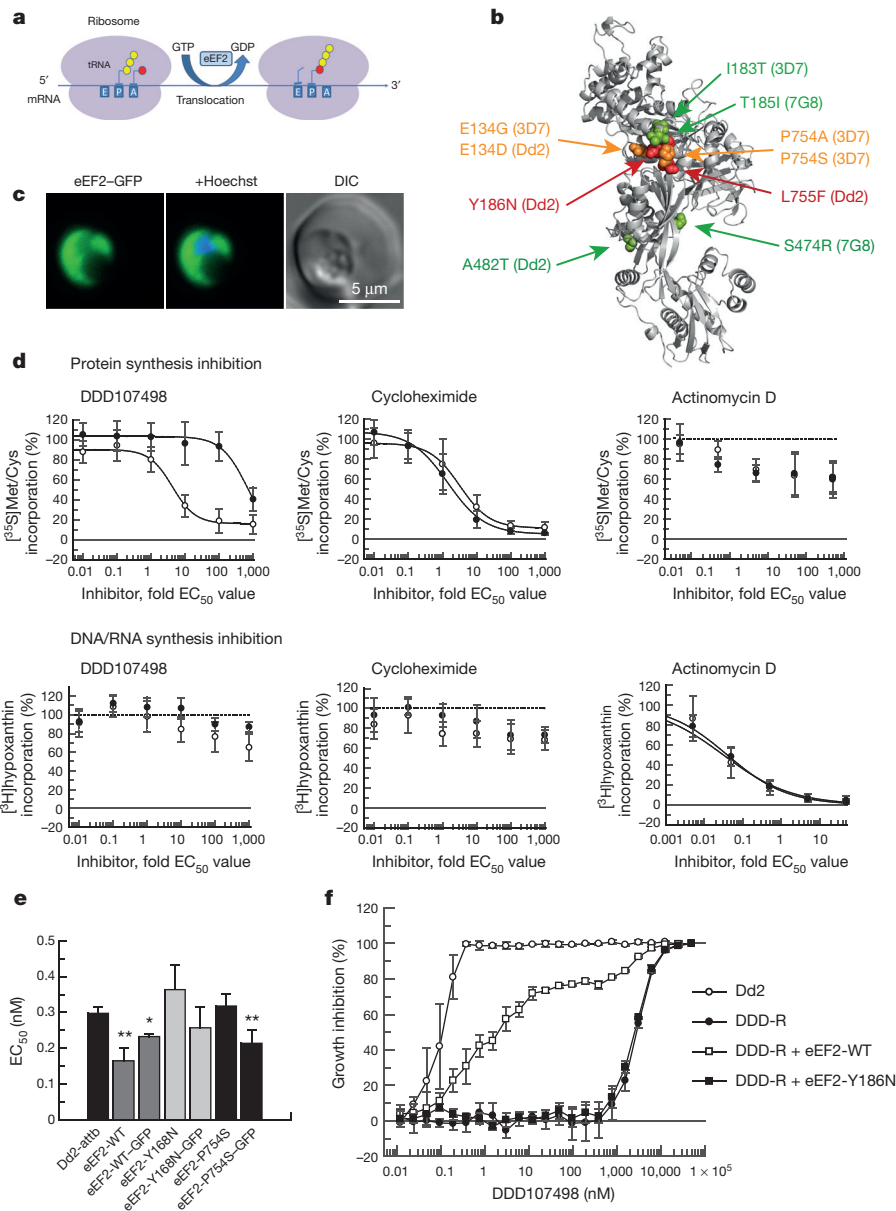


Figure 4 | DDD107498 targets protein synthesis via eEF2. **a**, eEF2 promotes the GTP-dependent translocation of the ribosome along messenger RNA during protein synthesis. **b**, Homology model of *P. falciparum* eEF2. The mapped mutations from each strain are colour coded by EC₅₀ fold (red, high; amber, moderate; green, low). **c**, Live-cell imaging of *P. falciparum* expressing an extra copy of eEF2 (WT) fused to GFP. The image is representative of more than 50 parasites visualized on two independent occasions. **d**, Protein and DNA/RNA synthesis were evaluated by measuring the incorporation of [³⁵S]Met/Cys (upper panel) and [³H]hypoxanthine (lower panel) into asynchronous 3D7 wild-type (open circles) and 3D7 DDD107498-resistant lines (eEF2-E134A/P754A) (filled circles) after incubation for 40 min with

encodes *P. falciparum* translation elongation factor 2 (PfeEF2). Three lines had two single nucleotide polymorphisms in PfeEF2, with a mixture of wild-type (WT) and mutant reads at each position (Supplementary Data 2), suggesting that these lines were mixtures of two clones, each with independent mutations in PfeEF2. Single nucleotide polymorphisms were confirmed by Sanger sequencing and nine validated mutations in PfeEF2 clustered in three regions of the encoded protein. In two cases identical single nucleotide polymorphisms were identified in two independent lines, indicating mutations in functionally important residues that were acquired independently in separate selection experiments. The fact that resistance

DDD107498, cycloheximide or actinomycin D. Radiolabelled incorporation, measured as counts per minute, was normalized as the percentage of incorporation against inhibitor concentration (means ± s.d.; *n* = 3 independent experiments, each run in duplicate). **e**, The EC₅₀ values for transfectants against DDD107498 (means ± s.d.; *n* = 4–7 independent experiments, each run in duplicate). Statistical significance was determined by the Mann–Whitney *U*-test: **P* < 0.05; ***P* < 0.01. **f**, DDD107498-resistant line (eEF2-Y186N) transfected episomally with plasmids expressing either WT eEF2 or eEF2-Y186N (means ± s.d.; *n* = 3 independent experiments, each run in duplicate).

to DDD107498 can be associated with multiple independent mutations is in keeping with observations from both artemisinin and other antimalarial compounds in development^{21–23}.

eEF2 is one of several essential elongation factors required in eukaryotic protein synthesis, by mediating GTP-dependent translocation of the ribosome along messenger RNA (mRNA) (Fig. 4a)²⁴. Yeast eEF2 is the target of the antifungal compound sordarin^{25,26}. Sordarin is selective for the *Saccharomyces cerevisiae* eEF2 over mammalian eEF2 *in vitro*, demonstrating that although protein synthesis in eukaryotes is conserved, it is possible to obtain selective inhibitors, despite the relatively high homology (67.2% identity) between the yeast and

human eEF2 (Extended Data Fig. 7)^{25,27}. In keeping with the potential for selectivity, DDD107498 is not toxic to mammalian cells (Extended Data Fig. 2c). The PfeEF2 mutations associated with resistance mapped to several areas on the surface of a homology model of the protein (on the basis of the structure of *S. cerevisiae* eEF2 with no ligands bound²⁸), with the mutations giving the highest degree of resistance clustering together (Fig. 4b). A DDD107498 binding pocket could not be elucidated through these modelling studies.

We confirmed that brief pre-incubation with DDD107498 specifically inhibited *P. falciparum* protein synthesis, by measuring short-term incorporation of [³⁵S]-labelled methionine and cysteine ([³⁵S]Met/Cys) in WT and DDD107498-resistant 3D7 *P. falciparum* parasites (Fig. 4d)²¹. Cycloheximide (a protein synthesis inhibitor) and DDD107498 both prevented [³⁵S]Met/Cys incorporation into WT *P. falciparum* 3D7, whereas actinomycin D (an inhibitor of RNA transcription) had minimal effect. Notably, DDD107498 was 100-fold less effective at inhibiting protein synthesis in DDD107498-resistant 3D7 than WT parasites, whereas cycloheximide prevented [³⁵S]Met/Cys incorporation equally in resistant and WT lines. DDD107498 and cycloheximide had minimal effects on DNA/RNA biosynthesis both in sensitive and in drug-resistant parasites (measured by incorporation of [³H]-labelled hypoxanthine), demonstrating specificity. In contrast, actinomycin D caused a marked dose-dependent reduction in [³H] incorporation.

To confirm that PfeEF2 is the target for DDD107498, we integrated transgenes expressing either WT PfeEF2 or resistance-associated alleles of PfeEF2 (Y186N, observed in mutant Dd2; and P754S, observed in mutant 3D7) using attPxattB integrase-mediated recombination^{21,29}. These transfectants also express endogenous PfeEF2. Imaging of green fluorescent protein (GFP)-fusions of PfeEF2 showed cytoplasmic localization (Fig. 4c), indicating that DDD107498 inhibits protein synthesis in the cytoplasm as opposed to the apicoplast³⁰, the site of action of tetracycline and azithromycin.

Dose-response assays with DDD107498 showed a similar inhibition profile between PfeEF2 transgene-expressing lines and the WT Dd2 strain, indicating that the endogenous WT PfeEF2 has a dominant effect in these experiments (Fig. 4e). This may be due to stable complex formation between the ribosome, WT PfeEF2 and DDD107498, resulting in ribosome stalling, which would explain why in mixed populations the WT PfeEF2 is dominant. For example in bacteria, fusidic acid binds to the complex between EF-G and the ribosome, preventing dissociation and blocking protein translation³¹.

To determine whether WT PfeEF2 was dominant in poisoning translation, we introduced episomal plasmids encoding WT or Y186N mutant PfeEF2 into the resistant PfeEF2 Y186N line (Fig. 4f). Plasmid-borne PfeEF2-Y186N had no effect on sensitivity to DDD107498 ($EC_{50} \approx 3,100$ nM), whereas WT PfeEF2 restored sensitivity ($EC_{50} = 2$ nM). This demonstrated a dominant effect of WT PfeEF2 on parasite susceptibility and confirmed that PfeEF2 is the primary molecular target of the compound. We note that the shallow slope observed for the WT PfeEF2 transfected line is probably a result of heterogeneous episomal plasmid copy number seen with episomally transformed parasite lines²⁹. Structural studies will be required to define precisely how DDD107498 interacts with eEF2 and the ribosome.

Resistance has been reported for all clinical antimalarials, including artemisinins². While the correlation between the rate of resistance generation in laboratory and clinical settings for antimalarials is not fully understood, it is important to evaluate the risk of all new antimalarials both in preclinical and in clinical studies. In our studies, the minimum inoculum for generating resistance to DDD107498 is within acceptable limits³². Furthermore, selected resistant Dd2 lines revealed impaired growth rates in the absence of drug pressure compared with WT Dd2 (Extended Data Fig. 8); moreover the higher the resistance, the greater the fitness defect. Importantly genome sequences from 1,685 clinical isolates of *P. falciparum* from 17 countries^{23,33} reveal

a high degree of PfeEF2 sequence conservation in the field. The sole non-synonymous single nucleotide polymorphism (T16S) identified was unique to West Africa (allele frequency of 0.002) and is in a PfeEF2 domain distinct from mutations associated with *in vitro* resistance to DDD107498.

Conclusion

DDD107498 represents a promising prospect for development as an antimalarial agent, with a potent activity profile against multiple life-cycle stages (sub-10 nM), a novel mode of action and excellent drug-like properties. It has potential for single-dose treatment, which has major implications for ensuring patient compliance and practical deployment. Its complementary activity on the sexual stages of the parasite has potential to reduce transmission and its action on the liver stage suggests a possible role in chemoprotection. Chemoprotection and transmission-blocking properties are fundamental to the goal of eliminating and eradicating malaria, for which the high potency and long half-life of DDD107498 are well suited.

Owing to general concerns about the emergence of resistance, all antimalarials are developed as combination therapies, a strategy shown to improve efficacy and reduce the development of drug resistance. In terms of treatment of the erythrocytic stage, DDD107498 fulfils the criteria as a long-duration partner to complete the clearance of blood-stage parasites¹¹. Therefore, it should be combined with a fast-acting compound, ideally with a pharmacological duration of action as close to DDD107498 as possible. This would reduce the initial level of infection, with the prolonged activity of DDD107498 eliminating the remaining parasites¹¹.

Inhibition of protein synthesis by DDD107498 through PfeEF2, which is expressed in multiple life-cycle stages³⁴, provides mechanistic support for the observed broad-spectrum profile. This highlights PfeEF2 as a novel drug target in malaria, and implies that inhibition of protein synthesis is an effective intervention for achieving multi-stage activity in *Plasmodium*. DDD107498 has now been progressed into advanced non-clinical development, with the aim of entering into human clinical trials.

Received 10 October 2014; accepted 7 April 2015.

- World Health Organization. *World Malaria Report 2014* (World Health Organization, 2014).
- Ariey, F. *et al.* A molecular marker of artemisinin-resistant *Plasmodium falciparum* malaria. *Nature* **505**, 50–55 (2014).
- Alonso, P. L. *et al.* A research agenda for malaria eradication: drugs. *PLoS Med.* **8**, e1000402 (2011).
- Wells, T. N. C. & Gutteridge, W. E. in *Neglected Diseases and Drug Discovery* (eds Palmer, M. J. & Wells, T. N. C.) Ch. 1 1–32 (Royal Society of Chemistry, 2012).
- Brenk, R. *et al.* Lessons learnt from assembling screening libraries for drug discovery for neglected diseases. *ChemMedChem* **3**, 435–444 (2008).
- Delves, M. *et al.* The activities of current antimalarial drugs on the life cycle stages of *Plasmodium*: a comparative study with human and rodent parasites. *PLoS Med.* **9**, e1001169 (2012).
- Russell, B. *et al.* Determinants of *in vitro* drug susceptibility testing of *Plasmodium vivax*. *Antimicrob. Agents Chemother.* **52**, 1040–1045 (2008).
- Karyana, M. *et al.* Malaria morbidity in Papua Indonesia, an area with multidrug resistant *Plasmodium vivax* and *Plasmodium falciparum*. *Malar. J.* **7**, 148 (2008).
- Angulo-Barturen, I. *et al.* A murine model of falciparum-malaria by *in vivo* selection of competent strains in non-myelodepleted mice engrafted with human erythrocytes. *PLoS ONE* **3**, e2252 (2008).
- Sanz, L. M. *et al.* *P. falciparum in vitro* killing rates allow to discriminate between different antimalarial mode-of-action. *PLoS ONE* **7**, e30949 (2012).
- Burrows, J. N., van Huijsduijnen, R. H., Mohrle, J. J., Oeuvray, C. & Wells, T. N. Designing the next generation of medicines for malaria control and eradication. *Malar. J.* **12**, 187 (2013).
- Meister, S. *et al.* Imaging of *Plasmodium* liver stages to drive next-generation antimalarial drug discovery. *Science* **334**, 1372–1377 (2011).
- Adjalley, S. H. *et al.* Quantitative assessment of *Plasmodium falciparum* sexual development reveals potent transmission-blocking activity by methylene blue. *Proc. Natl Acad. Sci. USA* **108**, E1214–E1223 (2011).
- Bousema, T. & Drakeley, C. Epidemiology and infectivity of *Plasmodium falciparum* and *Plasmodium vivax* gametocytes in relation to malaria control and elimination. *Clin. Microbiol. Rev.* **24**, 377–410 (2011).
- Delves, M. J. *et al.* Male and female *Plasmodium falciparum* mature gametocytes show different responses to antimalarial drugs. *Antimicrob. Agents Chemother.* **57**, 3268–3274 (2013).

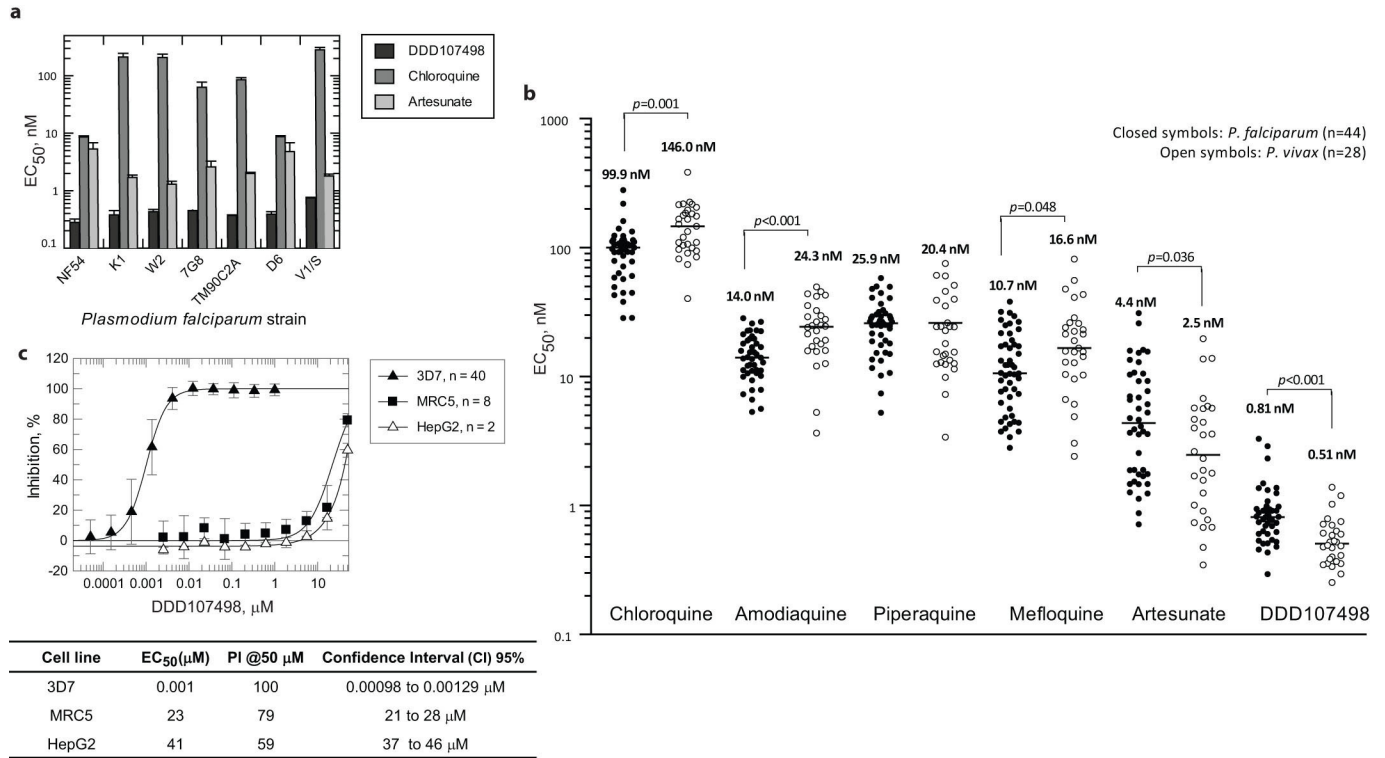
16. Delves, M. J. *et al.* A high-throughput assay for the identification of malarial transmission-blocking drugs and vaccines. *Int. J. Parasitol.* **42**, 999–1006 (2012).
17. Blagborough, A. M. *et al.* Transmission-blocking interventions eliminate malaria from laboratory populations. *Nature Commun.* **4**, 1812 (2013).
18. Upton, L. M. *et al.* Lead clinical and preclinical antimalarial drugs can significantly reduce sporozoite transmission to vertebrate populations. *Antimicrob. Agents Chemother.* **59**, 490–497 (2015).
19. Janse, C. J. *et al.* High efficiency transfection of *Plasmodium berghei* facilitates novel selection procedures. *Mol. Biochem. Parasitol.* **145**, 60–70 (2006).
20. Flannery, E. L., Fidock, D. A. & Winzeler, E. A. Using genetic methods to define the targets of compounds with antimalarial activity. *J. Med. Chem.* **56**, 7761–7771 (2013).
21. Rottman, M. *et al.* Spiroindolones, a potent compound class for the treatment of malaria. *Science* **329**, 1175–1180 (2010).
22. McNamara, C. W. *et al.* Targeting *Plasmodium* PI(4)K to eliminate malaria. *Nature* **504**, 248–253 (2013).
23. Miotto, O. *et al.* Multiple populations of artemisinin-resistant *Plasmodium falciparum* in Cambodia. *Nature Genet.* **45**, 648–655 (2013).
24. Jorgensen, R., Merrill, A. R. & Andersen, G. R. The life and death of translation elongation factor 2. *Biochem. Soc. Trans.* **34**, 1–6 (2006).
25. Justice, M. C. *et al.* Elongation factor 2 as a novel target for selective inhibition of fungal protein synthesis. *J. Biol. Chem.* **273**, 3148–3151 (1998).
26. Capa, L., Mendoza, A., Lavandera, J. L., de las Heras, F. G. & Garcia-Bustos, J. F. Translation elongation factor 2 is part of the target for a new family of antifungals. *Antimicrob. Agents Chemother.* **42**, 2694–2699 (1998).
27. Shastry, M. *et al.* Species-specific inhibition of fungal protein synthesis by sordarin: identification of a sordarin-specificity region in eukaryotic elongation factor 2. *Microbiology* **147**, 383–390 (2001).
28. Jorgensen, R. *et al.* Two crystal structures demonstrate large conformational changes in the eukaryotic ribosomal translocase. *Nature Struct. Biol.* **10**, 379–385 (2003).
29. Nkrumah, L. J. *et al.* Efficient site-specific integration in *Plasmodium falciparum* chromosomes mediated by mycobacteriophage Bxb1 integrase. *Nature Methods* **3**, 615–621 (2006).
30. Biswas, S. *et al.* Interaction of apicoplast-encoded elongation factor (EF) EF-Tu with nuclear-encoded EF-Ts mediates translation in the *Plasmodium falciparum* plastid. *Int. J. Parasitol.* **41**, 417–427 (2011).
31. Cox, G. *et al.* Ribosome clearance by FusB-type proteins mediates resistance to the antibiotic fusidic acid. *Proc. Natl Acad. Sci. USA* **109**, 2102–2107 (2012).
32. Ding, X. C., Ubben, D. & Wells, T. N. A framework for assessing the risk of resistance for anti-malarials in development. *Malar. J.* **11**, 292 (2012).
33. Manske, M. *et al.* Analysis of *Plasmodium falciparum* diversity in natural infections by deep sequencing. *Nature* **487**, 375–379 (2012).
34. Florens, L. *et al.* A proteomic view of the *Plasmodium falciparum* life cycle. *Nature* **419**, 520–526 (2002).
35. Jiménez-Díaz, M. B. *et al.* Quantitative measurement of *Plasmodium*-infected erythrocytes in murine models of malaria by flow cytometry using bidimensional assessment of SYTO-16 fluorescence. *Cytometry A* **75**, 225–235 (2009).
36. Charman, S. A. *et al.* Synthetic ozonide drug candidate OZ439 offers new hope for a single-dose cure of uncomplicated malaria. *Proc. Natl Acad. Sci. USA* **108**, 4400–4405 (2011).

Supplementary Information is available in the online version of the paper.

Acknowledgements This work was supported by grants from Medicines for Malaria Venture, the Wellcome Trust (100476 (I.H.G., A.H.F.), 091625 (R.N.P.) and 098051 (J.C.R., W.P., T.D.O.)), the Bill and Melinda Gates Foundation (OPP1043501 (M.D., R.S.)), the National Institutes of Health (R01 AI103058 to E.A.W. and D.A.F.) and the European Union (EVI-MalaR (T.D.O.)). Drug Discovery Unit infrastructure was supported by the European Regional Development Fund 2007–2013 and UK Research Partnership Investment Fund awards to M. Ferguson, whom we also thank for continued support. We thank C. Sibley for discussions. We acknowledge the East Scotland Blood Transfusion Service, Ninewells Hospital, Dundee, for erythrocyte supply to Dundee. We thank L. D. Shultz and The Jackson Laboratory for providing access to non-obese diabetic SCID IL2R γ c null mice through their collaboration with the GlaxoSmithKline Tres Cantos Medicines Development Campus. The following are acknowledged for technical assistance: all members of the Drug Discovery Unit (Dundee), M. Berriman, J. Kamber, E. Kenangalem, A. LaCrue, O. Montagnat, J. Rini Poespoprodjo, M. Sanders, S. Sax, C. Scheurer, L. Trianty, M. Tunnickliff (detailed in Supplementary Information).

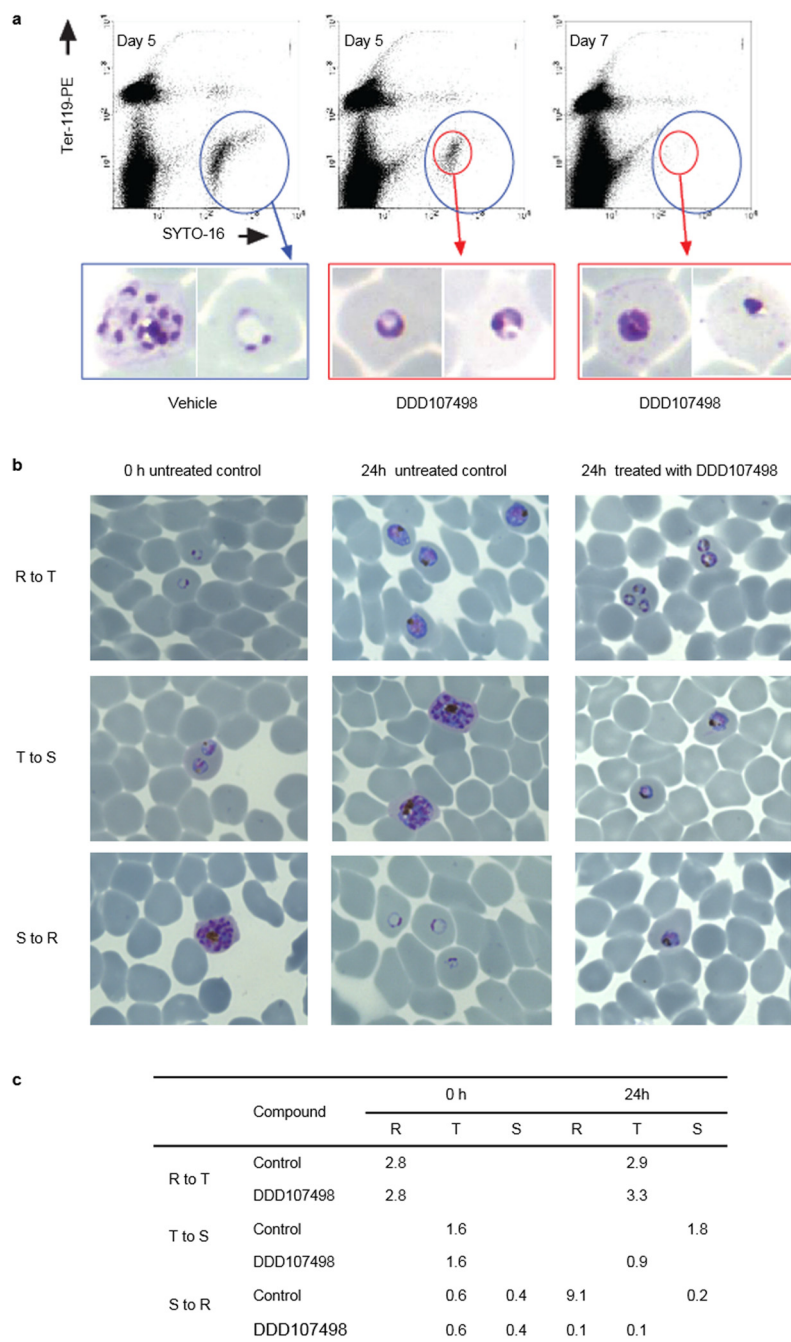
Author Contributions The author contributions are detailed in the Supplementary Information.

Author Information Reprints and permissions information is available at www.nature.com/reprints. The authors declare competing financial interests: details are available in the online version of the paper. Readers are welcome to comment on the online version of the paper. Correspondence and requests for materials should be addressed to I.H.G. (i.h.gilbert@dundee.ac.uk) or K.D.R. (k.read@dundee.ac.uk).



Extended Data Figure 2 | In vitro activity. **a**, *In vitro* activity against a panel of resistant and sensitive strains of *P. falciparum*. CQ, chloroquine; PYR, pyrimethamine; CYC, cycloguanil; QUI, quinine; SUL, sulfadoxine; MFQ, mefloquine. Resistance as follows: K1 (CQ, SUL, PYR, CYC); W2 (CQ, SUL, PYR, CYC); 7G8 (CQ, PYR, CYC); TM90C2A (CQ, PYR, MFQ, CYC); D6 (MFQ); V1/S (CQ, SUL, PYR, CYC). Data are the means \pm s.d. of $n = 3$

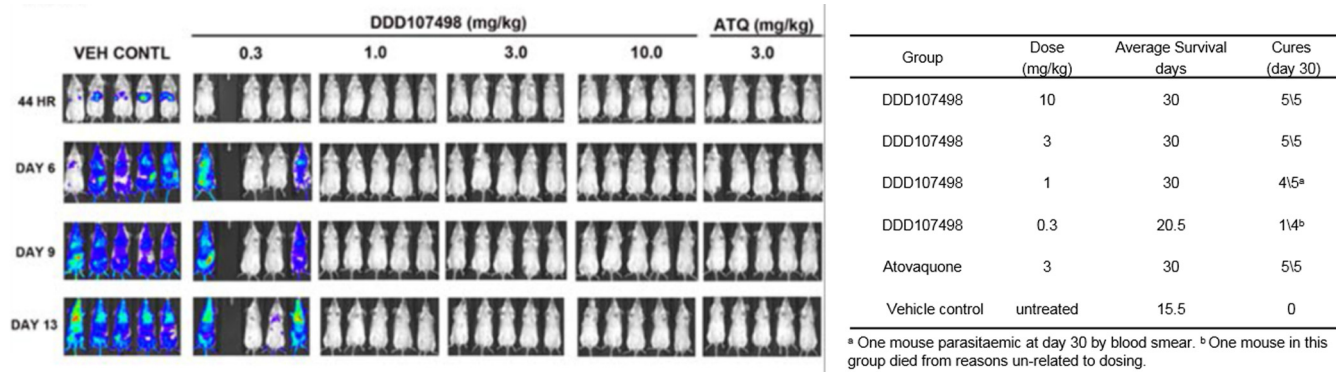
independent [³H]hypoxanthine incorporation experiments (each run in duplicate). **b**, *Ex vivo* activity against *P. falciparum* and *P. vivax* clinical isolates from Papua (Indonesia). The lines on the scatter plots represent the median value for each drug. **c**, Effect of DDD107498 on *P. falciparum* 3D7, HepG2 and MRC5 cells. Data are the means \pm s.d. of n reported independent experiments.



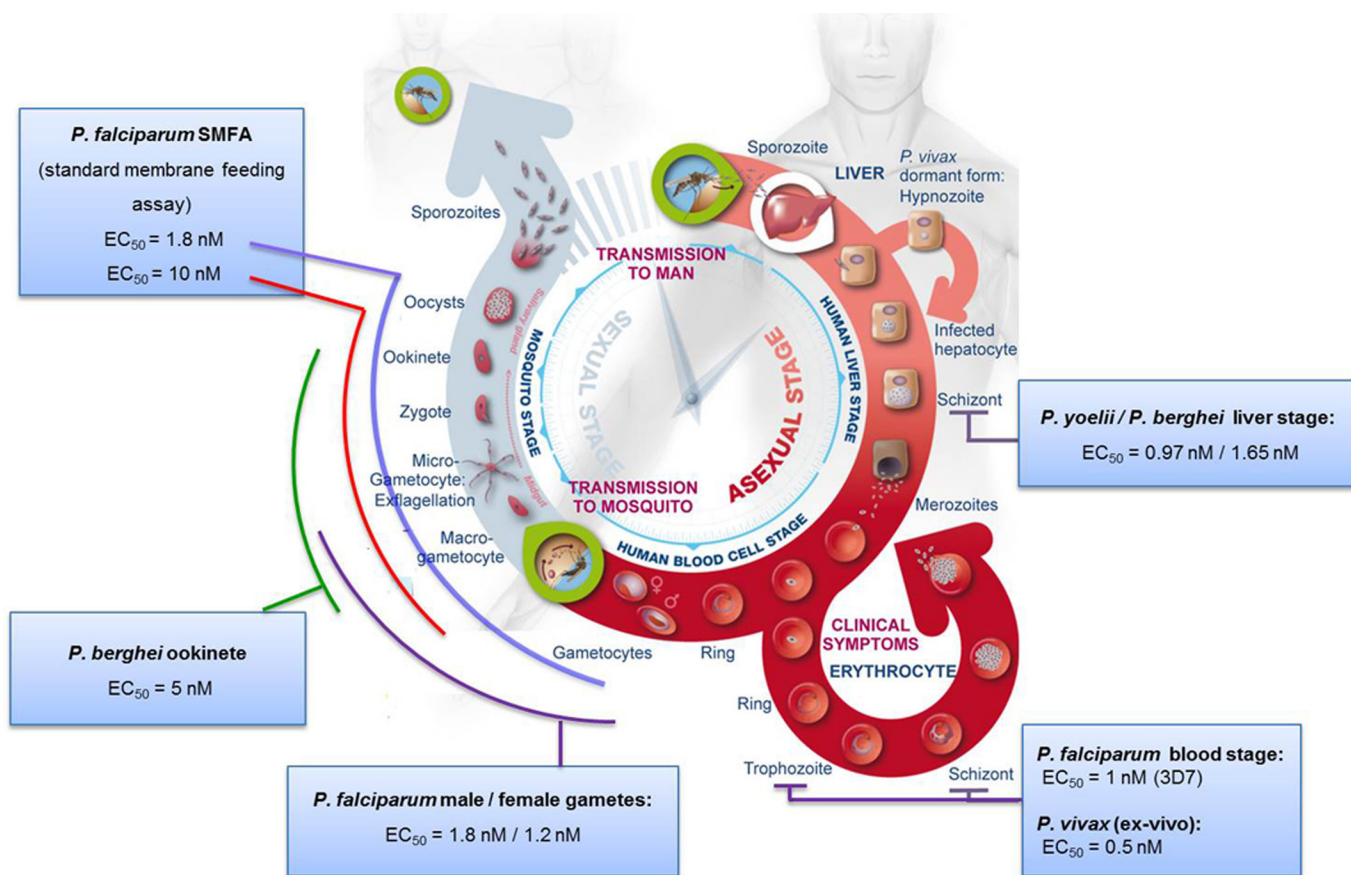
Extended Data Figure 3 | Effect of DDD107498 on parasite morphology.

a, Phenotype of *P. falciparum* in peripheral blood of NOD-*scid* IL-2R^{-null} mice engrafted with human erythrocytes. Blood samples were taken at days 5 and 7 of the assay (one and two asexual cycles, respectively) after the start of treatment with vehicle or DDD107498 at day 3. The bi-dimensional flow cytometry plots measure the murine (Ter-119-PE⁺) and human (Ter-119-PE⁻) erythrocytes, and the presence of nucleic acids (infected SYTO-16⁺ events). The blue circles indicate the region of infected erythrocytes. Vehicle-treated mice showed a characteristic pattern of staining with SYTO-16 (ref. 35), which correlated with the presence of healthy rings, trophozoites and schizonts in blood smears. Conversely, mice treated with DDD107498 at 50 mg per kg showed only trophozoites with condensed cytoplasm and some pyknotic cells at day 5 (red circle in flow cytometry plot and corresponding blood smears). By day 7, few infected erythrocytes were detected by flow cytometry and blood smears revealed parasites with a similar morphology to those at day 5. This suggests that trophozoites are the most sensitive population since the cycle is interrupted

at this stage. The images displayed are taken from a mouse with high levels of parasitaemia. At least 50 parasites were counted per sample screened in the microscope. Of these, four photographs of representative parasite phenotypes were selected to represent the morphology of the most prevalent phenotype. Thus, this is a qualitative assessment. **b**, Stage specificity assays using synchronized cultures. For morphological analysis of antimalarial drug action, thin blood smears were prepared, fixed and stained with Giemsa followed by examination with an upright microscope using an oil-immersion lens ($\times 100$). For parasitaemia determination, a total number of 1,000 red blood cells (corresponding to five microscopic fields) were counted. R to T, abnormal trophozoites observed after exposure for 24 h of synchronized rings to DDD107498. T to S, trophozoites do not develop into schizonts after exposure for 24 h to DDD107498. S to R, no ring stages are observed 24 h after treatment of schizonts with DDD107498. **c**, Percentage parasitaemia in the red blood cells. R, ring stage; T, trophozoite; S, schizont.



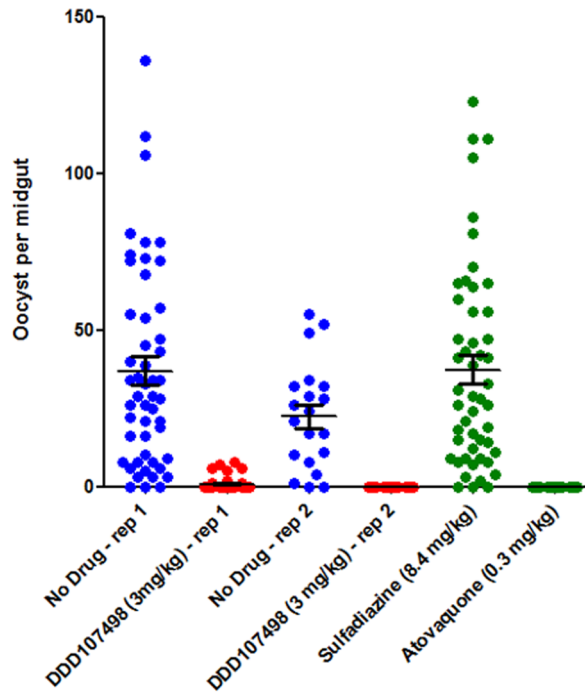
Extended Data Figure 4 | Prophylactic activity of DDD107498 against sporozoite challenge. *P. berghei* (luciferase) sporozoite *in vivo* mouse model of chemoprotection. A dose of 3 mg per kg was fully protective. Data are the mean of $n = 5$ experiments.



Extended Data Figure 5 | DDD107498 *in vitro* activity on the different life-cycle stages of *Plasmodium* spp. For comparator data with known antimalarials, see figure 5 in ref. 6. DDD107498 also showed potent activity *in*

vitro against *P. berghei* ookinetes¹⁶ (5.0 nM (95% CI 4.4–5.7 nM)), confirming that if DDD107498 was taken up during a blood meal, it could continue to kill parasites within the mosquito.

a



Intensity:	36.9	0.78	22.5	0	37.3	0
Prevalence:	94%	22%	90%	0%	94%	0%

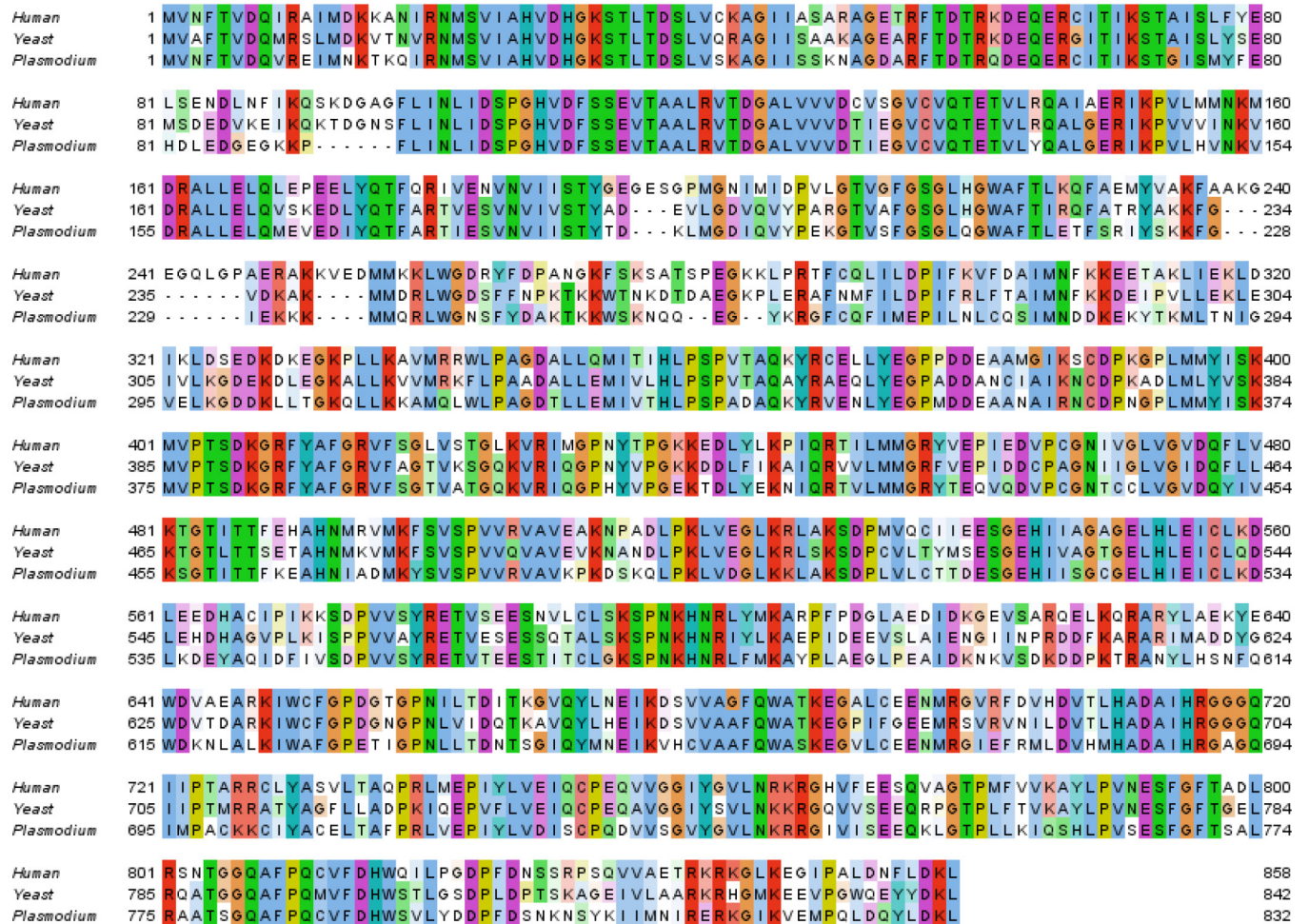
b

Effect on transmission to the mosquito host			
TB effect- oocyst intensity (%) (95% CIs)	TB effect- oocyst prevalence (%) (95% CIs)	TB effect- sporozoite intensity (%) (95% CIs)	TB effect- sporozoite prevalence (%) (95% CIs)
98.8% (98.1-99.3)	90.7% (72.9-97.2)	93.8% (88.7-96.6)	88.6% (78.3-94.2)
Effect on subsequent transmission to the vertebrate host			
Inhibition in infection of naive mice (%) (95% CIs)	Inhibition of parasitemia in infected mice (day 10 post-bite)	Effect size (95% CI)	
89.5% (71.4-100)	22.6%	90.5% (78.3-94.2)	

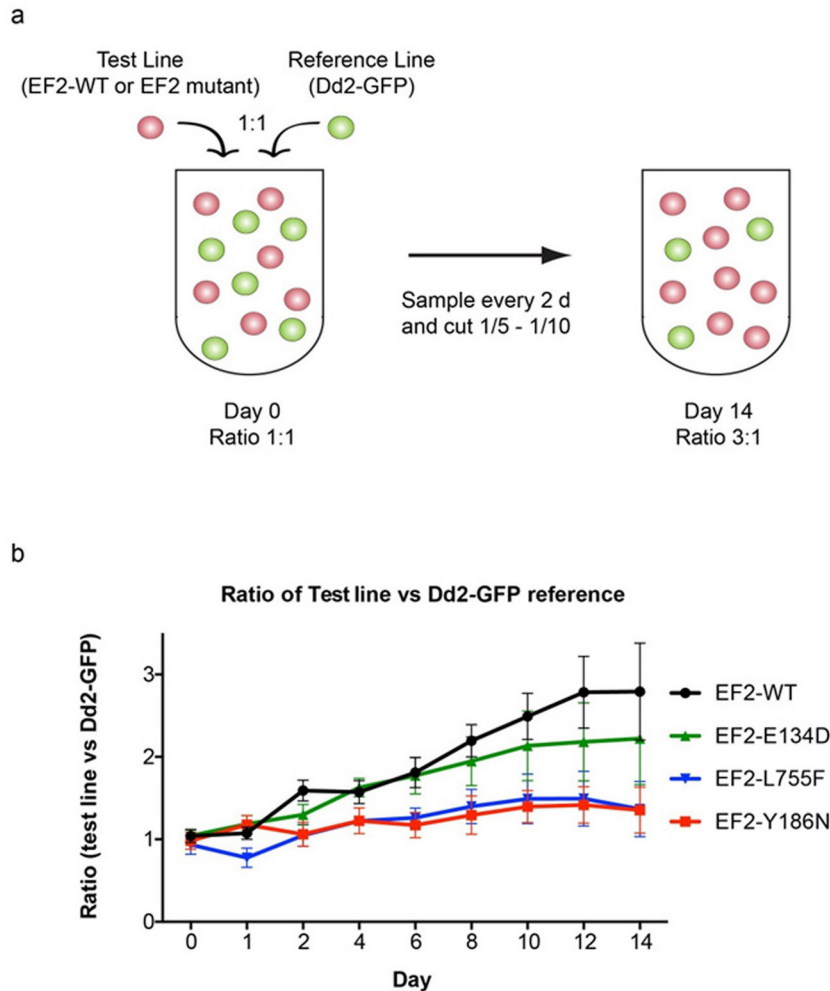
Extended Data Figure 6 | In vivo *P. berghei* mouse-to-mouse assay.

a, Impact of DDD107498 treatment on *in vivo* mosquito infection. Mice infected with *P. berghei* (PbGFPCON507 clone 1)¹⁹ were dosed orally with DDD107489 at 3 mg per kg, atovaquone at 0.3 mg per kg, sulphadiazine at 8.4 mg per kg, or were not drug treated (negative control). After 24 h, populations of treated mice (*n* = 5) were exposed to 500 female *Anopheles stephensi* mosquitoes, and oocyst intensity and infection prevalence in the mosquito midgut was measured 10 days after feeding. Individual data points represent the number of oocysts found in individual mosquitoes. Two replicates were performed. Sulphadiazine (8.4 mg per kg, intraperitoneally) and atovaquone (0.3 mg per kg, intraperitoneally) were used as negative and positive transmission-blocking drug controls, respectively. Horizontal bars represent mean intensity of infection, and error bars s.e.m., within individual mosquito populations. **b**, Impact of treatment with DDD107498 over a complete transmission cycle *in vivo*. After drug treatment of infected mice and mosquito

feeds, surviving potentially infectious mosquitoes were allowed to blood-feed on naive mice at a range of transmission settings (biting rates of 2, 5 and 10 bites per naive mouse) to assess the ability of drug treatment to reduce the number of new malarial cases after mosquito bite. Efficacy is expressed as the following: (1) impact on the mosquito population—expressed as reduction in both oocyst and sporozoite intensity and prevalence; (2) impact on subsequent transmission to new naive vertebrate hosts—expressed as reduction in infection of naive mice (reduction in number of new malarial cases after mosquito bite) and inhibition of subsequent parasitaemia (day 10 after bite) in mice that do become infected; (3) effect size generated—by fitting the data achieved within this assay to a chain-binomial model we could assess the ability of DDD107498 to reduce *R*₀ (assuming 100% coverage). If *R*₀ is reduced to <1, transmission is unsustainable and elimination will occur. Values of 95% CIs are shown in brackets. Efficacy is calculated in comparison with no-drug controls. TB, transmission blocking.



Extended Data Figure 7 | ClustalWS alignment of eEF2 sequences from human, yeast and *Plasmodium (P. falciparum)*. Alignment made using Jalview ClustalX default colouring.



Extended Data Figure 8 | Fitness phenotypes of DDD107498-resistant parasite lines. Unmarked Dd2- and DDD107498-selected parasites with various levels of resistance were assessed for growth in a competition assay, relative to a Dd2-GFP reference line. **a**, Equal numbers of unmarked test lines were mixed with the Dd2-GFP reference, in triplicate wells, and the ratio of non-fluorescent and fluorescent cells assessed by flow cytometry over time. At day 0, all lines had a 1:1 ratio with the Dd2-GFP reference. Increased growth of the test line over the Dd2-GFP reference, which has a slower growth rate than unmarked WT Dd2, would result in an increased ratio of test:Dd2-GFP.

b, Growth assay of four different test lines: (1) WT Dd2, (2) EF2-E134D, (3) EF2-L755F and (4) EF2-Y186N, relative to Dd2-GFP. A faster growth rate of WT Dd2 (DDD107498 IC_{50} 0.14 nM) relative to the fluorescent Dd2-GFP line is reflected in an increased ratio over time. The low-level resistant line EF2-E134D (IC_{50} 5.8 nM) did not attain a WT growth rate, and the high-level resistant lines EF2-L755F (IC_{50} 660 nM) and EF2-Y186N (3,100 nM) were further impaired. Means \pm s.d.; $n = 4$ independent experiments, each run in triplicate.

Extended Data Table 1 | Pharmacokinetics and rodent efficacy of DDD107498

a

	Mouse	Rat	Dog
Intravenous	1 mg/kg	1 mg/kg	1 mg/kg
Cl (ml/min/g)	12	18	30
V _{dss} (L/kg)	15	15	30
T _½ (h)	16	10	13
Oral	3 mg/kg	5 mg/kg	3 mg/kg
C _{max} (ng/ml)	90	180	27
T _{max} (h)	1	4	4
T _½ (h)	19	18	20
F%	74	84	46

b

Compound	30 mg/kg		10 mg/kg		3 mg/kg	
	Activity %	Survival days	Activity %	Survival days	Activity %	Survival days
Chloroquine [§]	99.9	10	99.5	7	83	7
Mefloquine [§]	99.6	22	95	16	<40	7
Artemether	98	7	89	6	59	6
Dihydroartemisinin	99	7	97	6	61	7
Artesunate [§]	92	9	75	6	<40	6
DDD107498	99.1	23	99.0	14	99	9

a. *In vivo* pharmacokinetic parameters in preclinical species ($n = 3$, all species). **b.** Oral *in vivo* single-dose efficacy of antimalarial drugs and DDD107498 in the murine *P. berghei* model. Data are the means of $n = 3$ for DDD107498 and $n \geq 5$ for the reference compounds. [§]Data from ref. 36.

Extended Data Table 2 | Summary of resistance selection experiments with DDD107498

Strain	Pressure (nM)	Pressure (x IC ₅₀)	Inoculum *						MIR	EC ₅₀ shift (inoculum)†
			Number of positive cultures (day of recrudescence)							
			10 ⁴	10 ⁵	10 ⁶	10 ⁷	10 ⁸	10 ⁹		
Dd2	1.25	2.7	ND	ND	2 (13, 41)	3 (13,13,15)	3 (13,13,16)	3 (29/29/29)	ND	2315 (10 ⁹) 7 (10 ⁸) 4810 (10 ⁸)
Dd2	1.25	2.7	0	0	0	3 (20,22,22)	ND	ND	10 ⁷	13 (10 ⁷)
Dd2	1.25	2.7	ND	0	1 (39)	ND	ND	ND	10 ⁸	5567 (10 ⁸)
7G8	1.25	3.1	ND	ND	0	3 (25, 25, 47)	1 (25)	3 (15,15,15)	10 ⁷	70 (10 ⁹) 60 (10 ⁸) 82 (10 ⁷)
3D7	1.5	3.3	ND	ND	0	2 (38, 38)	2 (28,28)	3 (20,20,20)	10 ⁷	19 (10 ⁹) 99 (10 ⁸) 14(10 ⁷)

*Number of positive cultures ($n = 3$) and day of recrudescence for each inoculum. †EC₅₀ fold change was determined on bulk cultures. MIR, minimum inoculum of resistance.